Proceedings of the 9th U.S. National and 10th Canadian Conference on Earthquake Engineering
Compte Rendu de la 9ième Conférence Nationale Américaine et
10ième Conférence Canadienne de Génie Parasismique
July 25-29, 2010, Toronto, Ontario, Canada • Paper No 1744

NEAR FIELD GROUND MOTION SYNTHESIS FOR GEMLIK REGION, TURKEY BASED ON SCENARIO EARTHQUAKES

G. Tanircan[1], C. Yenidogan[2] and N. Savas[3]

ABSTRACT

In this study, strong ground motion generations of Mw 6.9 scenario events of Gemlik fault was performed to broad-frequency (0.5-10 Hz) ground motion at 9 near-field stations.
In the first stage of the study, the focal mechanism of a small earthquake, which was used as the Green's function throughout the scenario simulation, was decided by simulating it with a smaller magnitude event. Several simulations have been performed using different fault mechanisms proposed for the event, the best waveform fitting was judged with the smallest misfit value.
In the second stage, near field ground motion simulation of scenario events from Gemlik fault was performed. Calculations were achieved for considering three different rupture scenarios which have the same magnitude but different asperity locations. The fault and asperity parameters for each scenario were determined from empirical scaling laws.
It has been found that for periods between 0.1 and 0.5 s, the design spectra were either nearly or actually exceeded by the scenario earthquakes. The majority of the structures in the area were built to lower design spectra before the 1998 code was implemented. Thus the strength of the many structures would have been insufficient to resist the forces that may be generated by an earthquake that is similar to the Scenario I. Calculated ground motion can be used as a design ground motion both for new projects and also for the emergency improvement of earthquake performance of structures. Hence, the results of the project is believed to serve to reduce the damage at both building and infrastructure due to a possible earthquake at Gemlik Bay.

Introduction

According to results of time dependent probabilistic hazard assessments for Turkey, the middle strand of the North Anatolian Fault (NAF) which passes through Iznik Lake to Bandirma has been found to be capable of producing the second highest hazard rate (PGA: 0.4-0.6g for bedrock) in the Marmara Region as compared to the Northern strands in Marmara Sea with the highest rate (Erdik et al, 2004). Although the slip rate and seismic activity are lower than those on Northern strand of NAF, recent investigations show that the fault segment extending between Gemlik-Bandirma (S41)

[1] Assist.Prof. Bogazici University, KOERI, Earthquake Engineering Department, Istanbul,TURKEY
[2] Res. Assist. Bogazici University, KOERI, Earthquake Engineering Department, Istanbul,TURKEY
[3] Ex-Grad.Student, Bogazici University, KOERI, Earthquake Engineering Department, Istanbul,TURKEY

and the Gemlik segment (S25) passing through the southern part of Iznik Lake have potentials of producing a magnitude 7 earthquake (Fig. 1, Fig. 2).

In the history, there have been several destructive earthquakes associated to these segments (Fig. 3). Recent paleoseismic studies have showed that two historic earthquakes, 1419 and 1857 earthquakes were occurred on Gemlik Segment (Ozalp et al, 2003). This finding states an existence of 589 year seismic gap at this region. Relative slip rate in the Gemlik Bay is given ~2-3mm/year (Straub et al.1997) suggesting a characteristic earthquake of magnitude 6.9 if the 40km segment ruptures at once. A comprehensive site response study for the Gemlik municipality indicates that PGA and PGV values may go up to 0.85g and 54cm/s due to the amplification of soil (Ansal et al, 2005). The concerned area between Yalova and Bursa accommodates dense urban and industrial areas and therefore it is necessary to prepare scenario earthquakes in order to understand the complexity of the ground shaking to be expected in a future earthquake and take action for future risk mitigation strategies.

The main objective of this study is to image scenario-based strong ground motion distribution between Yalova-Bursa areas where strong motion network was deployed. Calculated ground motion can be used as design ground motion both for new projects and also for the emergency improvement of earthquake performance of structures. Hence, the results of the project is believed to serve to reduce the damage at both building and infrastructure due to a possible earthquake at Gemlik Bay.

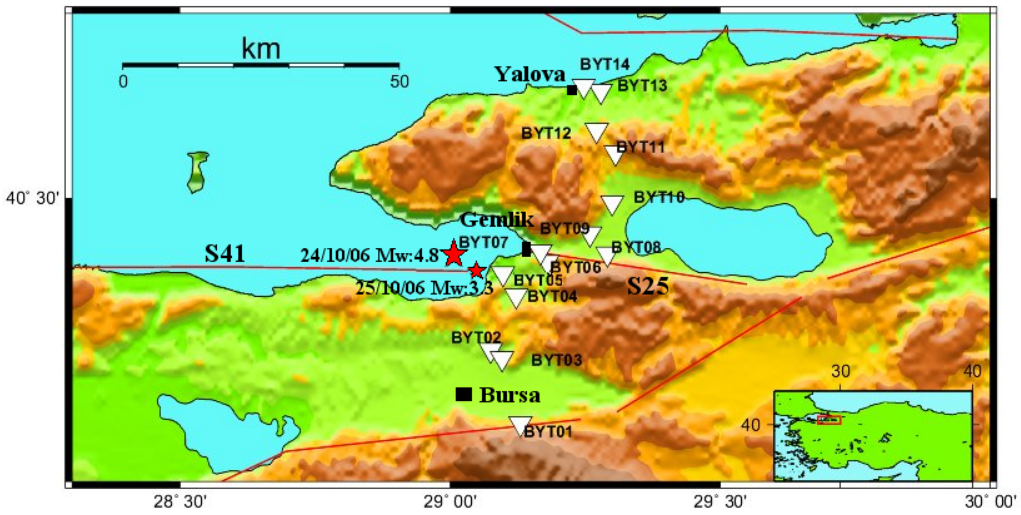

Figure 1. Location of BYTNet stations, fault segments S41 and S25 and earthquakes used as Green's functions.

Strong Motion Data

In the analysis, recordings from BYTNet *(*Bursa–Yalova Turkey Accelerograph Network*),* local accelerograph network encompassing 14 digital instruments were used (Fig. 3). Most of the stations used in the study are located on soft soil whose average shear wave velocity of the top 30m is around 300 m/s. Strong motion recordings of October 24 2006 (Mw:4.8) and October 25 2006 (Mw:3.3) earthquakes were used as the Green's Functions (Table 1). Acceleration waveforms were band-pass filtered in 0.5-10 Hz due to the signal-to-noise ratios of recordings. Since there is no information available

for the mechanism of the Mw:3.3 event, it was assumed to be the same as that of the Mw:4.8 event.

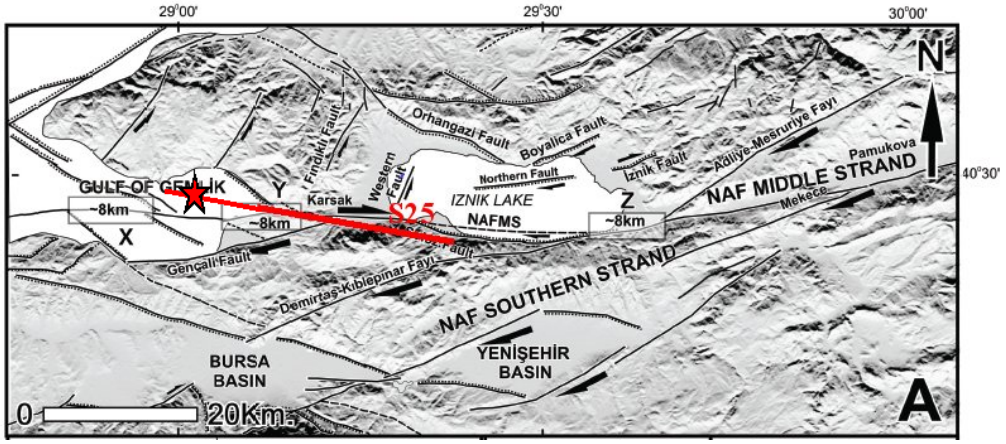

Figure 2 Active fault map of the Gemlik gegion (Ozturk et al, 2009).The assumed fault rupture of the scenario earthquakes are shown by a red line. The epicenter of the three scenarios is at the same place with Mw:4.8 earthquake.

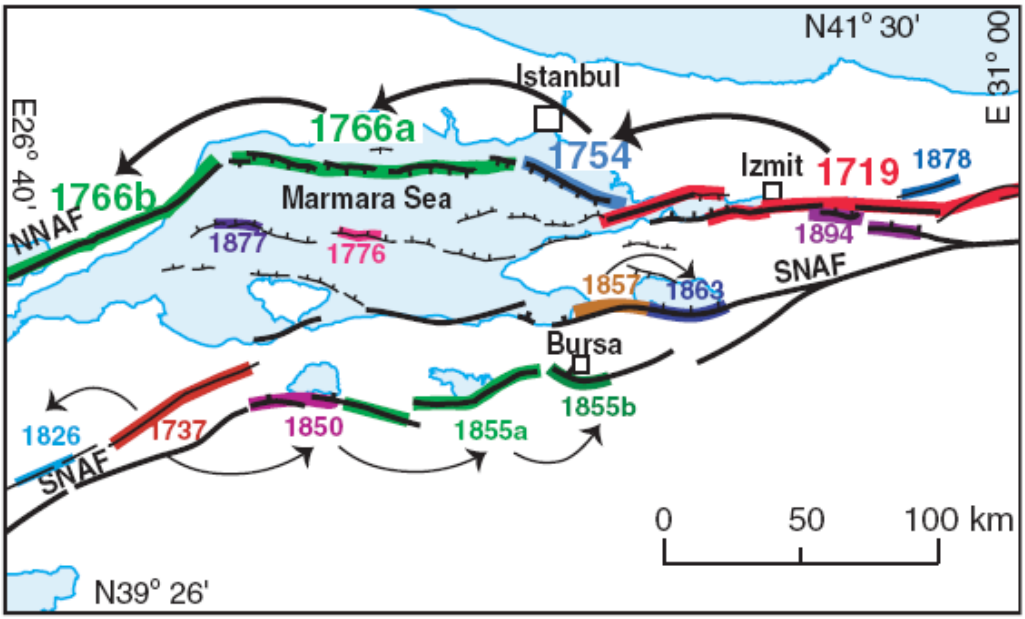

Figure 3. Historic earthquakes occurred between 1700 and 1900. (Hubert-Ferrari et al, 2000)

Table 1. Earthquake used in EGF simulation. Mw:3.3 event was used only for the simulation for focal mechanism confirmation of Mw:4.8 event.

Yr/Mo/Hr:Min(GMT)	Lat./Lon.	Depth	Mw
10-24-2006 (14:00)	40.422N - 28. 993E	20	4. 8
10-25-2006 (00.57)	40.413N - 29. 024E	10	3. 3

Ground Motion Synthesis

Simulation Method

Simulations were achieved by the method of Irikura (1986) which essentially uses the small events as the Empirical Green's Function (EGF) and sums them up to follow the omega squared scaling low. The main assumption is that the strong ground motion is generated only from asperities and each asperity has a nearly uniform stress drop. Asperities are divided into subfaults which are assumed to be point sources. One of the most important advantageous of the method is that site and propagation effect are already included in original recordings which is used as Green Functions and therefore method does not necessitates any modification of ground motion due to these effects.

Focal Mechanism Confirmation

Focal mechanism of the Mw:4.8 earthquake was reported by several agencies (Table 2). The fault plane solution determined by KOERI indicates that the rupture was right lateral strike slip on a northwest-southeast trending Gemlik Segment in Gemlik Bay. In a recent study, the focal mechanism of the Mw:4.8 earthquake was calculated with a different data set. Moment tensor solution of this study proposed a north-south oriented fault plane for the earthquake (Irmak et al., 2007).
In order to decide the appropriate focal mechanism, Mw: 4.8 event was synthesized by using Mw:3.3 event as the Green's Function (Table 3). Simulations were performed with the focal mechanisms solutions given by KOERI (strike/dip/rake: 317/86/-21) and Irmak et al (2007) (strike/dip/rake: 14/71/-12). The goodness of the fitting between observed and synthesized motions was judged by the displacement residuals calculated for different subfault size and rupture starting point. From two proposed focal mechanisms, simulation performed with focal mechanism provided by KOERI gave the smallest displacement residual sum and the best fitting for five BYTNET stations. For scenario simulations focal mechanism provided by KOERI were used as basis. In Fig. 4 observed and synthesized waveforms are presented.

Table 2. Source parameters of Mw:3.3 and 4.8 events found from EGF simulation

	Events	Corner Freq (Hz)	Rise Time (s)	Asperity size (km)
N:3	Mw:4.8	1.9	0.31	1.2 x1.1
C:12	Mw:3.3	4.3	0.23	0.4 x0.37

Scenario Simulation

Strong ground motion simulation of a Mw:6.9 characteristic earthquake in Gemlik Bay was performed assuming that a 40 km part of the Gemlik Segment will rupture. (Fig. 2). Hypocenter of the scenario earthquake was located between the segment S41 and western continuation of the Gemlik Segment in the Bay assuming that this region is one of the bending points of the NAF middle strand and possibility of rupture initiation is higher than those on the other parts of the fault segment. The rupture was initiated at a depth of 15 km for each of the scenario earthquakes.

Three different scenarios were defined by changing the asperity location. At each scenario a single asperity is assumed. In each asperity location of the rupture initiation was kept identical but rupture starting point was changed in order to investigate the near field effects. For Scenario I, II and III rupture starting point was located at the deep westernmost, center and easternmost of the asperity (Fig. 5), respectively.

The locations of the asperities in each fault plane are generally defined by considering the seismicity of the region, however due to the unavailability of accurate depth information of small events occurred at the concerned area for a long time span, following the Mai et al. (2005) and Manighetti et al. (2005) statements, each asperity was located at hypocenter region.

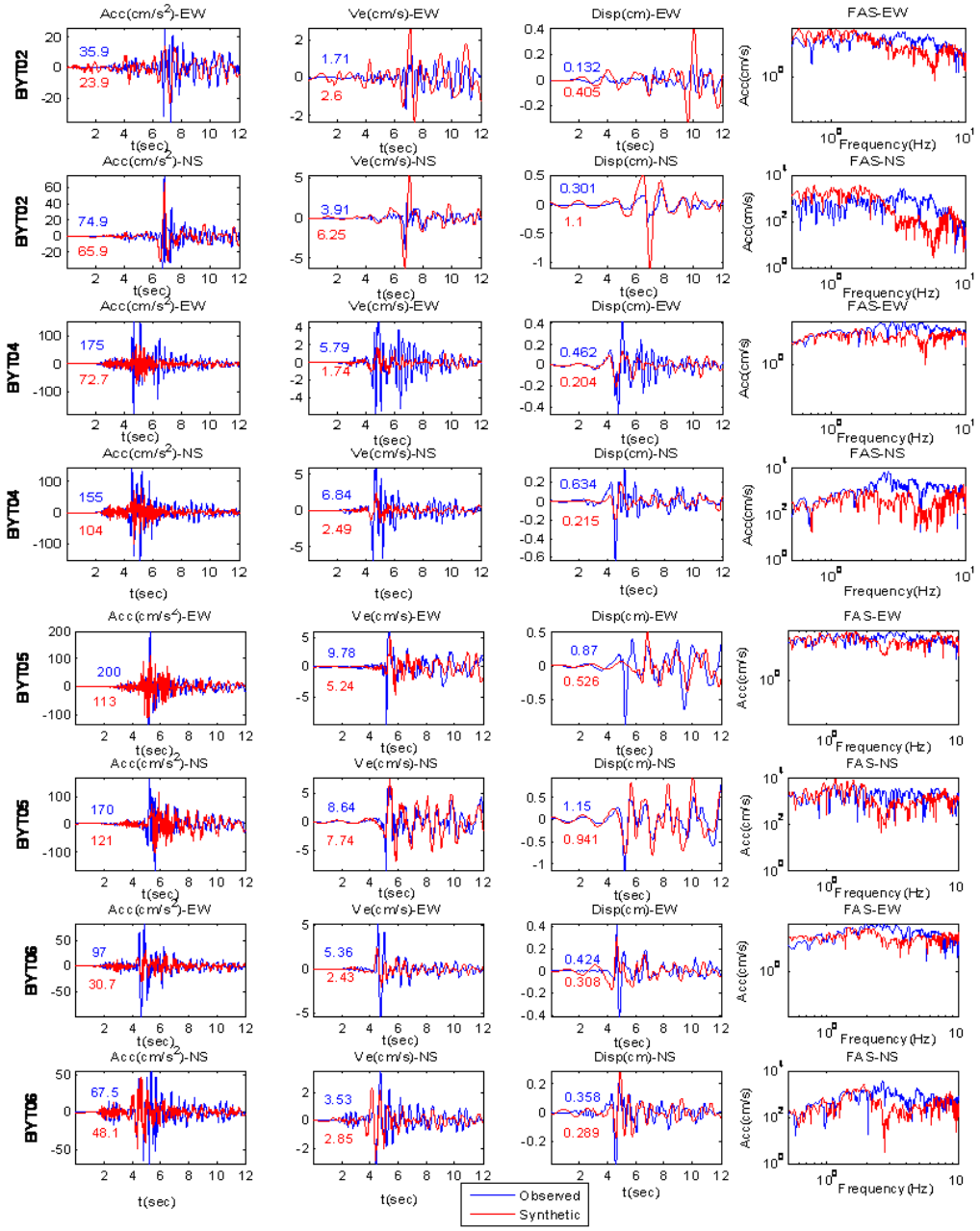

Figure 4. Comparison of observed and synthetic waveforms of acceleration, velocity, displacement and acceleration spectra for the Mw:4.8 Gemlik event, calculated at BYTNET stations with the focal mechanism solution provided by KOERI.

Source parameters of the simulation mainly follow the empirical scaling relationships of the Somerville et al (1999). Total seismic moment of 1.8e26dynecm was selected based on relationship of Hanks and Kanamori (1979). An average rupture velocity value of 2.8km/s was considered. Stress drop in asperity was calculated as 10 Mpa based on the relationship between seismic moment, average stress drop and asperity area as explained by Plido et al (2004). Asperity was subdivided to 10 x 9 subfaults, each representing the fault plane of Mw=4.8 earthquake.

Table 4. Asperity parameters

	Asperity Area (kmxkm)	**Number of Subfault**	**Rupture Vel.(km/sec)**	**Stress Drop (Mpa)**	M_0 **(Nm)**
Scenario 6.8	10 x 9	90	2.8	10.0	1.8e26

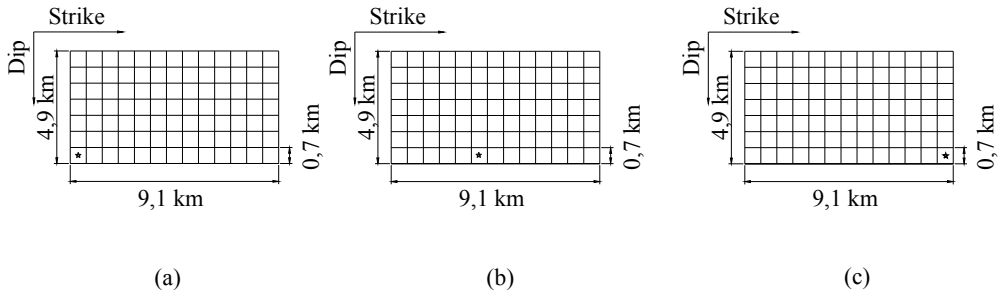

Figure 5. Rupture starting points at the beginning (a), middle (b) and end (c) of asperity for 6.9 scenario earthquake

Results

Near-fault ground motion time histories were calculated for nine BYTNET stations from each scenario. In all scenarios BYT05 station gives the maximum PGA and PGV values due to its close location to the rupture The PGA value reaches to 0.85g when rupture starting point was accepted at the beginning of the asperity (Scenario I), the rupture front propagates toward the site(toward the BYTNet stations), which in turn, is an omen of the forward rupture directivity. (Fig. 6). PGA values are in the limit of most recent NGA attenuation relationships that is also frequently used in Turkey. Ground motions from Scenario II and III and are smaller in amplitude and longer in duration when compared to that of Scenario I, since propagations were away from stations. Fig. 7 compares 5% damped acceleration response spectra from synthetic records calculated in scenario I with the design spectra drawn for Z2 and Z3 site classes accoring to the current Turkish Seismic Design Code (TSDC, 1997). In general, response spectra from TSDC exceed significantly the response spectra from the ground motions for shorter periods, except BYT04, BYT05 and BYT06 stations. In those stations ground motion exceeds the flat level of the design spectra particularly in the period range of 0.1-0.3sec.Significant spectral acceleration peaks at 0.2 and 0.3sec at BYT01-BYT06 stations are clear.

At longer periods the rupture directivity effect is manifested in a peak at about 1.5 to 2 s in the NS component acceleration response spectrum of BYT07 and BYT08. In most ground motions forward directivity effect is absent since stations are apparently too close to epicenter for directivity effects to built up .

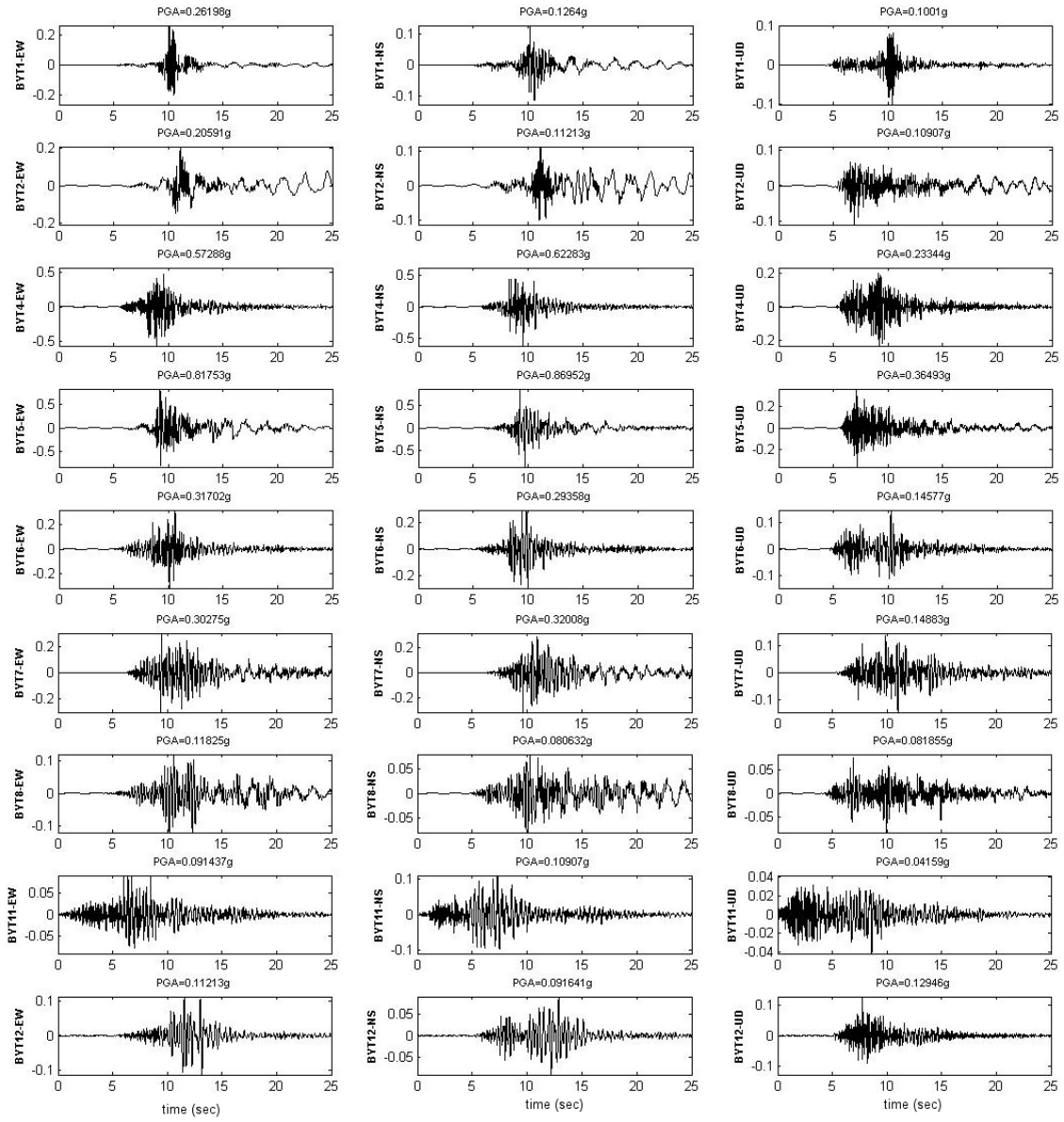

Figure 6 Synthetic ground motions for the Scenario I

Table 5 Peak PGA and PGV values from scenario earthquakes.

	Scenario I				Scenario II				Scenario III			
	PGA(g)		PGV(cm/s)		PGA(g)		PGV(cm/s)		PGA(g)		PGV(cm/s)	
Stations	**N-S**	**E-W**	**N-S**	**E-W**	**N-S**	**E-W**	**N-S**	**E-W**	**N-S**	**E-W**	**N-S**	**E-W**
BYT01	0.26	0.12	10.9	7.52	0.08	0.08	4.12	3.21	0.07	0.05	2.81	1.83
BYT02	0.20	0.11	20.5	11.4	0.12	0.07	8.97	6.08	0.12	0.07	8.48	4.93
BYT04	0.56	0.61	18.5	21.4	0.37	0.40	18.3	16.8	0.30	0.33	10.4	11.8
BYT05	0.80	0.85	53.4	37.2	0.67	0.43	58	37.4	0.37	0.30	21.6	19.2
BYT06	0.31	0.29	14.6	15.2	0.16	0.18	7.54	9.42	0.14	0.17	8.33	10.3
BYT07	0.30	0.31	11.1	14.1	0.26	0.36	10.1	11.9	0.24	0.25	13.3	11.8
BYT08	0.12	0.08	9.35	7.03	0.11	0.13	8.66	9.5	0.08	0.10	6.88	8.33
BYT11	0.09	0.11	3.49	5.66	0.11	0.10	3.41	5.13	0.06	0.08	1.86	3.61
BYT12	0.11	0.09	6.44	4.75	0.08	0.07	4.83	4.54	0.09	0.07	4.79	3.5

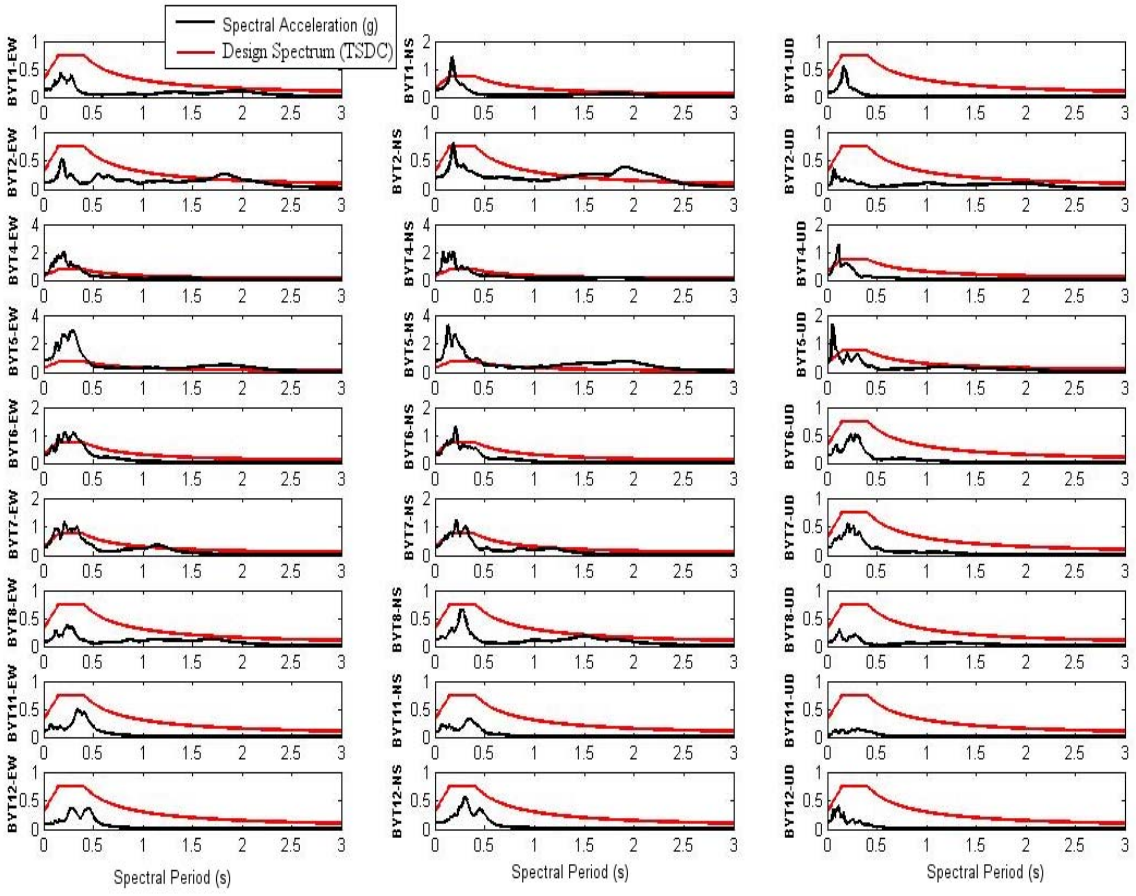

Figure 7 Comparison between simulated acceleration response spectra and the current Turkish Seismic Design Code (TSDC) at stations for the Scenario I.

Conclusions

In the present study a deterministic hazard at Gemlik Bay was evaluated based on finite rupture models. In the first step, the focal mechanism of a small earthquake, which was used as the Green's function throughout the scenario simulation, was decided by simulating it with a smaller magnitude event. In the second step, near field ground motion simulation of scenarios from Gemlik-Bandirma and Iznik fault segments were performed. Calculations were achieved for considering three different rupture scenarios. The fault and asperity parameters for each scenario were determined from empirical scaling laws. Results have been evaluated in time histories of acceleration, velocity and spectral response acceleration. Results are generally in agreement with earlier probabilistic hazard studies performed for this region (Erdik et al, 2004 Ansal et al, 2006).

In general, design spectra of TSDC exceed the response spectra from the ground motions for shorter periods, except the nearest stations. At those stations source and site effects significantly increase the ground motion, as well as response spectral acceleration in short periods. As illustrated in acceleration response spectra graphs, for periods between 0.1 and 0.5 s, the design spectra were either nearly or actually exceeded by the scenario earthquakes. The majority of the structures in the area were built to lower design spectra before the 1998 code was implemented. Thus the strength of the many structures would have been insufficient to resist the forces that may be generated by an earthquake that is similar to the Scenario I. Calculated ground motion can be used as a design ground motion both for new projects and also for the emergency improvement of earthquake performance of structures. Hence, the results of the project is believed to serve to reduce the damage at both building and infrastructure due to a possible earthquake at Gemlik Bay.

References

Ansal A., Tonuk G., Bayraklı Y.,(2005b). Microzonation for site conditions for Bakirkoy, Gemlik, Bandirma, Tekirdag, Eskisehir and Korfez. WB Meer Project-A3 Component, Microzonation and hazard vulnerability studies for disaster mitigation in pilot municipalities.

Boore, D.M., Joyner, W.B and Fumal, T.E. (1997). Equations for estimating horizontal response spectra and peak acceleration from Western North American earthquakes: a summary of recent work. *Seismological Research Letters* 68:1, 128-153.

Erdik, M., Demircioglu, M., Sesetyan, K., Durukal, E. and Siyahi, B. (2004). Earthquake hazard in Marmara Region, Turkey. *Soil Dynamics and Earthquake Engineering* 24:8, 605-631.

Hanks, T.C. and Kanamori, H. (1979). A moment magnitude scale. *Journal of Geophysical Research* 84:2, 2348-2350.

Hubert-Ferrari., A., Barka, A., Nalbant S., Meyer, B., Armijo, R., (2000), 17 Ağustos 1999 depremi sonrasında Marmara'da deprem riski. *Bilim ve Teknik*, 389, 54 – 58.

Irikura, K. (1986). Prediction of strong acceleration motion using Empirical Green's function. Proceedings 7th Japan Earthquake Engineering Symposium, Tokyo, 151-156.

Irikura, K. and Miyake, H. (2003). Lecture notes on strong motion seismology.

http://www.kojiro-irikura.jp/english.html.

Irmak, T.S., Grosser, H., Özer, M.F., Woith, H. and Baris, S. (2007). The 24 October 2006 Gemlik Earthquake (M=5.2). *Geophysical Research Abstracts* 9, 10212.

Mai, P.M., Spudich, P. and Boatwright, J. (2005). Hypocenter locations in finite-source rupture models. *Bulletin of the Seismological Society of America* 95:3, 965-980.

Manighetti, I., Campillo, M., Sammis, C., Mai, P.M. and King, G. (2005). Evidence for self-similar, triangular slip distributions on earthquakes: implications for earthquakes and fault mechanics. *Journal of Geophysical Research* 110, 5302.

Ozturk, K., Yaltirak C., Alpar B. (2009). The relationship between the tectonic setting of the lake İznik Basin and the middle strand of the North Anatolian fault. *Turkish J. Earth Sci*., 18, 209-224.

Pulido, N., Ojeda, A., Atakan, K. and Kubo, T. (2004). Strong ground motion estimation in the sea of Marmara region (Turkey) based on a scenario earthquake. *Tectonophysics* 391, 357– 374.

Straub, C., Kahle, H.G. and Schindler, C. (1997). GPS and geologic estimates of the tectonic activity in the Marmara Sea region NW Anatolia. *J. Geoph. Res.-Solid Earth*, B12, 27587−27601

Ozalp S., Dogan A., Emre O. (2003).The last two faulting events on the southern strand of the North Anatolian Fault Zone, NW Turkey, AGU 2003 Fall meeting.

Turkish Seismic Design Code(2007). “Specifications For Buildings to be Built In Seismic Areas”, in Turkish, Ministry of Public Works and Settlement, Ankara, Turkey.